

# ANOMALOUS RESISTIVITY AND THE ORIGIN OF HEAVY MASS IN THE TWO-BAND HUBBARD MODEL WITH ONE NARROW BAND

*M. Yu. Kagan*<sup>a\*</sup>, *V. V. Val'kov*<sup>b</sup>

<sup>a</sup>*Kapitza Institute for Physical Problems  
119334, Moscow, Russia*

<sup>b</sup>*Kirenskii Institute of Physics  
660036, Krasnoyarsk, Russia*

Received November 1, 2010

**Dedicated to the memory of Professor A. G. Aronov**

We search for marginal Fermi-liquid behavior [1] in the two-band Hubbard model with one narrow band. We consider the limit of low electron densities in the bands and strong intraband and interband Hubbard interactions. We analyze the influence of electron polaron effect [2] and other mechanisms of mass enhancement (related to momentum dependence of the self-energies) on the effective mass and scattering times of light and heavy components in the clean case (electron–electron scattering and no impurities). We find the tendency towards phase separation (towards negative partial compressibility of heavy particles) in the 3D case for a large mismatch between the densities of heavy and light bands in the strong-coupling limit. We also observe that for low temperatures and equal densities, the homogeneous state resistivity  $R(T) \sim T^2$  behaves in a Fermi-liquid fashion in both 3D and 2D cases. For temperatures higher than the effective bandwidth for heavy electrons  $T > W_h^*$ , the coherent behavior of the heavy component is totally destroyed. The heavy particles move diffusively in the surrounding of light particles. At the same time, the light particles scatter on the heavy ones as if on immobile (static) impurities. In this regime, the heavy component is marginal, while the light one is not. The resistivity saturates for  $T > W_h^*$  in the 3D case. In 2D, the resistivity has a maximum and a localization tail due to weak-localization corrections of the Altshuler–Aronov type [3]. Such behavior of resistivity could be relevant for some uranium-based heavy-fermion compounds like  $\text{UNi}_2\text{Al}_3$  in 3D and for some other mixed-valence compounds possibly including layered manganites in 2D. We also briefly consider the superconductive (SC) instability in the model. The leading instability is towards the  $p$ -wave pairing and is governed by the enhanced Kohn–Luttinger [4] mechanism of SC at low electron density. The critical temperature corresponds to the pairing of heavy electrons via polarization of the light ones in 2D.

## 1. INTRODUCTION

The physics of uranium-based heavy-fermion compounds and the origin of a heavy mass  $m_h^* \sim 200m_e$  for  $f$ -electrons in them is possibly very different (see [2]) from the physics of cerium-based heavy fermions, where the Kondo effect (or more generally, the physics of the Kondo lattice model) is dominant [5, 6]. The point is that uranium-based heavy fermions are usually in the mixed-valence limit [7] with strong hybridization between heavy ( $f$  electrons or  $f-d$  electrons) and light

( $s-p$  electrons) components. On the level of two-particle hybridization, the interband Hubbard interaction leads to an additional enhancement of the heavy electrons mass due to the electron polaron effect (EPE). Physically, the EPE is connected with a nonadiabatical part of the many-body wave function describing a heavy electron and a cloud of virtual electron–hole pairs of light particles. These pairs are mixed with the wave function of the heavy electron but do not follow it when a heavy electron tunnels from one elementary cell to a neighboring one. It is shown in [2] that in the unitary limit of the strong Hubbard interaction between heavy and light electrons, the effective heavy mass can

---

\*E-mail: kagan@kapitza.ras.ru

reach the value  $m_h^*/m_L \sim (m_h/m_L)^2$ , and if we start from the ratio  $m_h/m_L \sim 10$  between bare masses of heavy and light electrons, on the level of LDA approximation, for example, we could finish with the effective value  $m_h^* \sim 100m_L$ , which is typical for uranium-based heavy-fermion compounds.

A similar effect can also be described using strong one-particle hybridization between heavy and light bands [2].

A natural question arises whether the two-band Hubbard model with one narrow band is a simple toy model to observe non-Fermi liquid behavior and the well-known marginal Fermi liquid behavior in particular [1]. We recall that in the marginal Fermi liquid (MFL) theory, the quasiparticles are strongly damped ( $\text{Im}\varepsilon \sim \text{Re}\varepsilon \sim T$ ). According to [1], the strong damping  $\gamma \sim T$  of quasiparticles (instead of the standard damping  $\gamma \sim T^2/\varepsilon_F$  for a Landau–Fermi liquid) can explain numerous experiments in HTSC compounds including a linear resistivity  $R(T) \sim T$  for  $T > T_C$  at optimal doping concentrations. The MFL picture was also proposed to describe the properties of UPt<sub>3</sub> doped by Pd including the specific heat measurements [8]. We note that the two-band Hubbard model with one narrow band is a natural generalization of the well-known Falicov–Kimball model [9] but contains richer physics due to a finite width of the heavy band (instead of a localized level), which allows an interesting dynamics of the heavy component.

In this paper, we evaluate the damping and transport times for heavy and light electrons. We test these times for marginality and find that for low temperatures  $T < W_h^*$  ( $W_h^*$  is the effective bandwidth for heavy electrons) and equal densities of heavy and light bands in a homogeneous state, we have the standard Landau–Fermi liquid behavior with a resistivity  $R(T) \sim T^2$  in the case of electron–electron scattering in both 3D and 2D. For higher temperatures  $T > W_h^*$  ( $W_h^* \sim 50$  K for  $m_h^* \sim 200m_e$ ), the heavy band is totally destroyed and heavy particles move diffusively in the surrounding of light particles, while the light particles scatter on the heavy ones as if on immobile (static) impurities. For these temperatures, the heavy component is marginal, but the light one is not. We try to find a marginal behavior of the light component with weak localization corrections of the Altshuler–Aronov type [3] for the scattering time of light electrons taken into account. We do not obtain a marginal behavior of the light component, but we obtain a very interesting anomalous resistivity characteristics, especially in the 2D case, where the resistivity has a maximum

for  $T \sim W_h^*$  and a localization tail at higher temperatures [10]. In 3D, the resistivity saturates for  $T > W_h^*$ . Such resistivity characteristics could possibly describe some 3D uranium-based heavy-fermion compounds like UNi<sub>2</sub>Al<sub>3</sub> and some other mixed-valence systems including Yb-based heavy-fermion compounds [11, 12], where the low-density approach pursued in this paper could possibly describe the real experimental situation. In 2D, the behavior of resistivity possibly has some relation to layered manganites, where we deal with two degenerate ( $e_g$ ) conducting orbitals (bands) of d electrons of Mn. However, an alternative explanation is possible for manganites [13]. According to it, the resistivity is governed by electron tunneling from one metallic FM polaron to a neighboring one via an insulating AFM or PM barrier in the regime of nanoscale phase separation in the electron subsystem. It would be interesting to compare these two mechanisms for resistivity in layered manganites in more detail.

We also consider other mechanisms of heavy mass enhancement different from the EPE and find a very pronounced effect in 3D connected with a momentum dependence of the self-energy of heavy electrons due to the “heavy–light” interaction. In the strong-coupling limit, this effect could provide even larger ratios of  $m_h^*/m_h$  than the EPE does. It leads to negative compressibility of heavy particles and thus reveals the tendency towards phase separation or at least charge redistribution between the bands for a large density mismatch  $n_h \gg n_L$ , in qualitative agreement with the results in [14].

In the final section, we study the leading SC instability that arises in the two-band model in the 2D case. The leading instability at low density is proved to be towards the triplet  $p$ -wave pairing. It describes the pairing of heavy electrons via polarization of light electrons [15, 16] in the framework of the enhanced Kohn–Luttinger [4] mechanism of SC and provides rather realistic critical temperatures in the 2D or layered case, especially for the situation of geometrically separated bands belonging to neighboring layers.

## 2. THE TWO-BAND HUBBARD MODEL WITH ONE NARROW BAND

The Hamiltonian of the two-band Hubbard model is given by

$$\begin{aligned}
\hat{H}' = & -t_h \sum_{\langle ij \rangle \sigma} a_{i\sigma}^+ a_{j\sigma} - t_L \sum_{\langle ij \rangle \sigma} b_{i\sigma}^+ b_{j\sigma} - \\
& - \varepsilon_0 \sum_{i\sigma} n_{i\sigma}^h - \mu \sum_{i\sigma} (n_{i\sigma}^L + n_{i\sigma}^h) + \\
& + U_{hh} \sum_i n_{ih}^\uparrow n_{ih}^\downarrow + U_{LL} \sum_i n_{iL}^\uparrow n_{iL}^\downarrow + \\
& + \frac{U_{hL}}{2} \sum_i n_{iL} n_{ih}, \quad (1)
\end{aligned}$$

where  $U_{hh}$  and  $U_{LL}$  are intraband Hubbard interactions for heavy and light electrons respectively  $U_{hL}$  is the interband Hubbard interaction between heavy and light electrons,  $t_h$  and  $t_L$  are transfer integrals for heavy and light electrons,  $n_{i\sigma}^\sigma = a_{i\sigma}^+ a_{i\sigma}$ ,  $n_{i\sigma}^L = b_{i\sigma}^+ b_{i\sigma}$  are the densities of heavy and light electrons on site  $i$  with spin projection  $\sigma$ , and  $\mu$  is the chemical potential. We note that  $-\varepsilon_0$  is the center of gravity of the heavy band, and the difference  $\Delta$  between the bottoms of the bands is given by

$$\Delta = -\varepsilon_0 + \frac{W_L - W_h}{2} = E_{min}^h - E_{min}^L.$$

After the Fourier transformation, we obtain

$$\begin{aligned}
\hat{H}' = & \sum_{p\sigma} \varepsilon_h(p) a_{p\sigma}^+ a_{p\sigma} + \sum_{p\sigma} \varepsilon_L(p) b_{p\sigma}^+ b_{p\sigma} + \\
& + U_{hh} \sum_{pp'q} a_{p\uparrow}^+ a_{p'\downarrow}^+ a_{p-q\downarrow} a_{p'+q\uparrow} + \\
& + U_{LL} \sum_{pp'q} b_{p\uparrow}^+ b_{p'\downarrow}^+ b_{p-q\downarrow} b_{p'+q\uparrow} + \\
& + \frac{U_{hL}}{2} \sum_{\substack{pp'q \\ \sigma\sigma'}} a_{p\sigma}^+ (b_{p'\sigma'}^+ b_{p-q\sigma'}) a_{p'+q\sigma}, \quad (2)
\end{aligned}$$

where in  $D$  dimensions for the hypercubic lattice,

$$\varepsilon_h(p) = -2t_h \sum_{a=1}^D \cos(p_a d) - \varepsilon_0 - \mu$$

and

$$\varepsilon_L(p) = -2t_L \sum_{a=1}^D \cos(p_a d) - \mu$$

are the quasiparticle energies for heavy and light bands (see Fig. 1), and  $p_a = \{p_x, p_y, \dots\}$  are Cartesian projections of the momentum. For low densities of heavy and light components  $n_{tot} d^D = (n_h + n_L) d^D \ll 1$ , the quasiparticle spectra are

$$\begin{aligned}
\varepsilon_h(p) = & -\frac{W_h}{2} + t_h(p^2 d^2) - \varepsilon_0 - \mu, \\
\varepsilon_L(p) = & -\frac{W_L}{2} + t_L(p^2 d^2) - \mu, \quad (3)
\end{aligned}$$

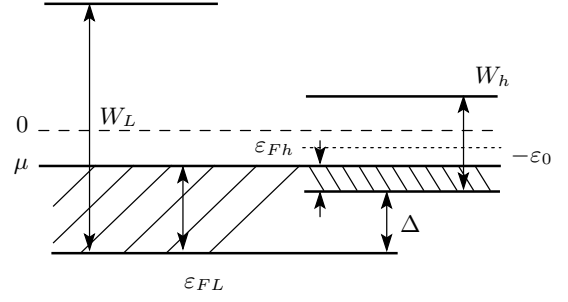


**Fig. 1.** Band structure in the two-band model with one narrow band.  $W_h$  and  $W_L$  are the bandwidths of heavy and light electrons,  $\varepsilon_{Fh}$  and  $\varepsilon_{FL}$  are the Fermi energies,  $\Delta = -\varepsilon_0 + (W_L - W_h)/2$  is the energy difference between the bottoms of the heavy and light bands, with  $(-\varepsilon_0)$  being the center of gravity of the heavy band. The center of gravity of the light band is at zero.  $\mu$  is chemical potential

where  $W_h = 4Dt_h$  and  $W_L = 4Dt_L$  are the bandwidths of heavy and light electrons for the  $D$ -dimensional hypercubic lattice and  $d$  is the intersite distance. Hence, introducing the bare masses of heavy and light components

$$m_h = \frac{1}{2t_h d^2}, \quad m_L = \frac{1}{2t_L d^2} \quad (4)$$

and Fermi energies

$$\varepsilon_{Fh} = \frac{p_{Fh}^2}{2m_h} = \frac{W_h}{2} + \mu + \varepsilon_0, \quad \varepsilon_{FL} = \frac{W_L}{2} + \mu, \quad (5)$$

we finally obtain the quasiparticle spectra for  $T \rightarrow 0$  as

$$\varepsilon_h(p) = \frac{p^2}{2m_h} - \varepsilon_{Fh}, \quad \varepsilon_L(p) = \frac{p^2}{2m_L} - \varepsilon_{FL}. \quad (6)$$

In deriving (4)–(6) we implicitly assumed that the difference between the bottom of the bands  $\Delta$  in Fig. 1 is not too large, and hence the parabolic approximation for the spectra of both bands is still valid. We note that there is no one-particle hybridization in Hamiltonians (1) and (2), but there is a strong two-particle hybridization

$$\frac{U_{hL}}{2} \sum_i n_i^h n_i^L.$$

We assume that  $m_h \gg m_L$ , and therefore

$$W_h/W_L = m_L/m_h \ll 1. \quad (7)$$

We also assume that the strong-coupling situation  $U_{hh} \sim U_{LL} \sim U_{hL} \gg W_L \gg W_h$  occurs ( $U_{hL}$  is large because in reality light particles experience strong scattering on the heavy ones as if on a quiresonance level). Finally we consider the simplest case where the densities of the bands are of the same order:  $n_h \sim n_L$  (in 3D,  $n = p_F^3/3\pi^2$ , while in 2D,  $n = p_F^2/2\pi$ ).

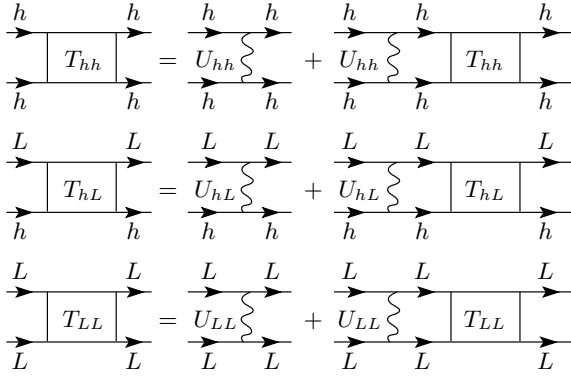


**Fig. 2.**  $T$ -matrices  $T_{hh}$ ,  $T_{LL}$ , and  $T_{hL}$  for the two-band model with heavy ( $h$ ) and light ( $L$ ) electrons,  $U_{hh}$  and  $U_{LL}$  are the intraband Hubbard interactions, and  $U_{hL}$  is the interband Hubbard interaction between heavy and light particles

### 3. THE KANAMORI $T$ -MATRIX APPROXIMATION

According to the renormalization scheme of Kanamori, the strong Hubbard interactions [17] in the case of low electron density (almost empty lattice) should be described in terms of the corresponding vacuum  $T$ -matrices (see Fig. 2). In the 3D case, the solution of the corresponding Bethe–Salpeter integral equations in the vacuum yields for the  $T$ -matrices (see [15–17])

$$T_{hh} = \frac{U_{hh}d^3}{1 - U_{hh}d^3 K_{hh}^{vac}(0,0)} \approx \frac{U_{hh}d^3}{1 + U_{hh}/8\pi t_h}, \quad (8)$$

$$T_{hL} \approx \frac{U_{hL}d^3}{1 + U_{hL}/8\pi t_{hL}^*}, \quad T_{LL} \approx \frac{U_{LL}d^3}{1 + U_{LL}/8\pi t_L},$$

where

$$K_{hh}^{vac}(0,0) \approx - \int \frac{d^3\mathbf{p}}{(2\pi)^3} \frac{m_h}{p^2}$$

is a Cooper loop for heavy particles in the vacuum (the product of two vacuum Green's functions of heavy particles in a Cooper channel for the total frequency and total momentum equal to zero),

$$m_{hL}^* = \frac{1}{2t_{hL}^*d^2} = \frac{m_h m_L}{m_h + m_L} \approx m_L$$

for  $m_h \gg m_L$  is an effective mass for the  $T$ -matrix  $T_{hL}$  (for scattering of light electrons on heavy ones) and, accordingly,  $t_{hL}^* \approx t_L$  is an effective transfer integral;  $Ud^3$  plays the role of the zeroth Fourier component in 3D. As a result, for  $U_{hh} \sim U_{LL} \sim U_{hL} \gg W_L \gg W_h$ , we have

$$T_{hh} \approx 8\pi t_h d^3, \quad T_{hL} \approx T_{LL} \approx 8\pi t_L d^3. \quad (9)$$

The  $s$ -wave scattering length for the Hubbard model [15] is defined as  $a = mT/4\pi = T/8\pi t d^2$ , and hence

$$a_{hh} = a_{hL} = a_{LL} \approx d \quad (10)$$

in the strong-coupling case.

Correspondingly, the gas parameter of Galitskii  $f_0 = 2ap_F/\pi$  [18, 19] in the case of equal densities of heavy and light bands  $n_L = n_h$  is given by

$$f_0 = (f_0^L \approx 2dp_{FL}/\pi) = (f_0^h \approx 2dp_{Fh}/\pi) \approx \approx 2dp_F/\pi \quad (11)$$

(it is convenient to include the factor  $2/\pi$  in the definition of the gas parameter in 3D). In the 2D, case for strong Hubbard interactions and low densities, with logarithmic accuracy, the vacuum  $T$ -matrices for  $n_L = n_h$  are given by [15, 16]

$$T_{hh} \approx \frac{U_{hh}d^2}{1 + \frac{U_{hh}}{8\pi t_h} \int_{\sim p_F^2}^{\sim 1/d^2} \frac{dp^2}{p^2}} \approx \frac{U_{hh}d^2}{1 + \frac{U_{hh}}{8\pi t_h} \ln \frac{1}{p_F^2 d^2}}, \quad (12)$$

$$T_{LL} \approx \frac{U_{LL}d^2}{1 + \frac{U_{LL}}{8\pi t_L} \ln \frac{1}{p_F^2 d^2}},$$

$$T_{hL} \approx \frac{U_{hL}d^2}{1 + \frac{U_{hL}}{8\pi t_L} \ln \frac{1}{p_F^2 d^2}},$$

where  $Ud^2$  plays the role of the zeroth Fourier component of the Hubbard potential in 2D. As a result, in the strong-coupling case, the 2D gas parameter of Bloom [20] for equal densities  $n_L = n_h$  is

$$f_0 = f_{0L} = f_{0h} \approx \frac{1}{2 \ln(1/p_F d)}. \quad (13)$$

### 4. EVALUATION OF THE SELF-ENERGIES OF HEAVY AND LIGHT BANDS

We evaluate the imaginary part  $\text{Im} \Sigma$  of self-energies in the two-band Hubbard model considering the clean case (no impurities) and taking only the electron–electron scattering into account. It is important for evaluation of the scattering times for heavy and light electrons and the subsequent calculation of the resistivity  $R(T)$ . In the two-band model (see Fig. 3),

$$\Sigma_h = \Sigma_{hh} + \Sigma_{hL} \quad \text{and} \quad \Sigma_L = \Sigma_{LL} + \Sigma_{Lh}. \quad (14)$$

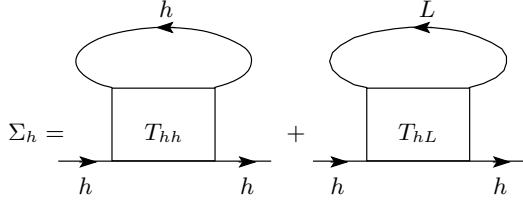


**Fig. 3.** The  $T$ -matrix approximation for the self-energy of a heavy particle.  $T_{hh}$  and  $T_{hL}$  are the full  $T$ -matrices in substance. The diagrams for  $\Sigma_L$  are similar

In the 3D case, the full  $T$ -matrices in substance that enter in the diagrams for  $\Sigma_{hh}$  in Fig. 3 have the form

$$T_{hh}(\Omega, \mathbf{p}) = \frac{U_{hh}d^3}{1 - U_{hh}d^3K_{hh}(\Omega, \mathbf{p})}, \quad (15)$$

where

$$K_{hh}(\Omega, \mathbf{p}) = \int \frac{d^3\mathbf{p}'}{(2\pi)^3} \frac{1 - n_h^F(\varepsilon_{p'+p}) - n_h^F(\varepsilon_{-p'})}{\Omega - \varepsilon_h(p'+p) - \varepsilon_h(-p') + i0} \quad (16)$$

is a Cooper loop in substance (the product of two Green's functions in the Cooper channel),  $n_h^F(\varepsilon)$  is the Fermi–Dirac distribution function for heavy particles, and similarly for the full  $T$ -matrices  $T_{hL}$ ,  $T_{Lh}$ , and  $T_{LL}$  and Cooper loops  $K_{hL}$ ,  $K_{Lh}$ , and  $K_{LL}$ .

If we expand the  $T$ -matrix for heavy particles in the first two orders in the gas parameter, then according to Galitskii [18] we obtain

$$T_{hh}(\Omega, \mathbf{p}) = \frac{4\pi a_h}{m_h} + \left(\frac{4\pi a_h}{m_h}\right)^2 (K_{hh} - K_{hh}^{vac}) + o\left[\left(\frac{4\pi a_h}{m_h}\right)^3 (K_{hh} - K_{hh}^{vac})^2\right], \quad (17)$$

where

$$\frac{4\pi a_h}{m_h} \approx \frac{U_{hh}d^3}{1 - U_{hh}d^3K_{hh}^{vac}} \quad (18)$$

coincides with the Kanamori approximation for the vacuum  $T$ -matrix and

$$K_{hh}^{vac}(\Omega, \mathbf{p}) \approx \int \frac{d^3\mathbf{p}'/(2\pi)^3}{\Omega - \frac{(\mathbf{p} + \mathbf{p}')^2}{2m_h} - \frac{p'^2}{2m_h}}$$

is the Cooper loop in the vacuum (rigorously speaking, the scattering length is defined by  $K_{hh}^{vac}(0, 0)$ , but the difference between  $K_{hh}^{vac}(\Omega, \mathbf{p})$  and  $K_{hh}^{vac}(0, 0)$  is proportional to the gas parameter  $a_h p_{Fh}$  and is small).  $K_{hh}$  in (17) is the full Cooper loop (cooperon) in substance for heavy particles given by (16). If we consider

low densities and the energies close to  $\varepsilon_F$ , we can show that the terms neglected in  $T_{hh}$  are small with respect to the gas parameter

$$\frac{4\pi a_h}{m_h} (K_{hh} - K_{hh}^{vac}) \sim a_h p_{Fh}.$$

The self-energy of heavy particles  $\Sigma_{hh}$  in the first two orders of the gas parameter is given by

$$\Sigma_{hh}(p) = \sum_k T_{hh}(k+p)G_h(k) \approx \frac{4\pi a_h}{m_h} \sum_k G_h(k) - \left(\frac{4\pi a_h}{m_h}\right)^2 \sum_k (K_{hh} - K_{hh}^{vac})G_h(k) + o(a_h p_{Fh})^3. \quad (19)$$

The first term becomes  $4\pi a_h n_h/m_h$ , which is just the Hartree–Fock contribution. In the second term, we can make an analytic continuation  $i\omega_n \rightarrow \omega + i0$  for the bosonic propagator  $K_{hh}$  and the fermionic propagator  $G_h$ . As a result (bearing in mind that  $\text{Im} K_{hh}^{vac} = 0$ ), we obtain the imaginary part of  $\Sigma_{hh}^{(2)}$  as

$$\begin{aligned} \text{Im} \Sigma_{hh}^{(2)}(\varepsilon, \mathbf{p}) &= \left(\frac{4\pi a_h}{m_h}\right)^2 \times \\ &\times \sum_k \text{Im} K_{hh}(\varepsilon_k + \varepsilon, \mathbf{k} + \mathbf{p}) [n_B(\varepsilon_k + \varepsilon) + n_F(\varepsilon_k)] = \\ &= -\left(\frac{4\pi a_h}{m_h}\right)^2 \pi \int \frac{d^3\mathbf{k}}{(2\pi)^3} \int \frac{d^3\mathbf{p}'}{(2\pi)^3} \times \\ &\times [1 - n_h^F(\mathbf{p} + \mathbf{p}' + \mathbf{k}) - n_h^F(-\mathbf{p}')] \times \\ &\times [n_B(\varepsilon_k + \varepsilon) + n_F(\varepsilon_k)] \times \\ &\times \delta[\varepsilon + \varepsilon_h(\mathbf{k}) - \varepsilon_h(\mathbf{p} + \mathbf{p}' + \mathbf{k}) - \varepsilon_h(-\mathbf{p}')] \quad (20) \end{aligned}$$

and similarly for the real part of  $\Sigma_{hh}^{(2)}$ :

$$\begin{aligned} \text{Re} \Sigma_{hh}^{(2)}(\varepsilon, \mathbf{p}) &= \left(\frac{4\pi a_h}{m_h}\right)^2 \times \\ &\times \sum_k [\text{Re} K_{hh}(\varepsilon_k + \varepsilon, \mathbf{k} + \mathbf{p}) - \\ &- \text{Re} K_{hh}^{vac}(\varepsilon_k + \varepsilon, \mathbf{k} + \mathbf{p})] \times \\ &\times [n_B(\varepsilon_k + \varepsilon) + n_F(\varepsilon_k)], \quad (21) \end{aligned}$$

where for the real part of a Cooper loop in vacuum,

$$\begin{aligned} \text{Re} K_{hh}^{vac}(\varepsilon_k + \varepsilon, \mathbf{k} + \mathbf{p}) &= \int \frac{d^3\mathbf{p}'}{(2\pi)^3} \times \\ &\times P \frac{2m_h}{\mathbf{k}^2 + \mathbf{p}^2 - (\mathbf{p}' + \mathbf{k} + \mathbf{p})^2 - p'^2} \quad (22) \end{aligned}$$

is calculated at resonance for  $\Omega = \varepsilon_k + \varepsilon_p$  (or for  $\varepsilon = \varepsilon_p$ ), and  $P$  is the principal value. In (20) and (21),  $n_B(\Omega) = 1/(e^{\Omega/T} - 1)$  and  $n_F(\Omega) = 1/(e^{\Omega/T} + 1)$  are the bosonic and fermionic distribution functions, and hence

$$n_B(\varepsilon_k + \varepsilon) + n_F(\varepsilon_k) = \frac{1}{2} \left[ \text{cth} \frac{\varepsilon_k + \varepsilon}{2T} - \text{th} \frac{\varepsilon_k}{2T} \right]. \quad (23)$$

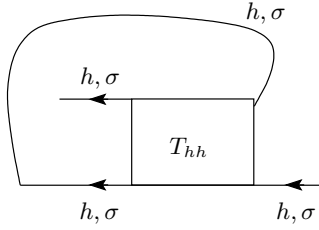


**Fig. 4.** An exchange-type diagram for the self-energy  $\Sigma_{hh}^\sigma$  that contains the matrix element  $a_\sigma^+ a_\sigma^+ a_\sigma a_\sigma$  and is therefore absent in the Hubbard model

The real part of the Cooper loop in substance for heavy particles is given by

$$\text{Re } K_{hh}(\varepsilon_k + \varepsilon, \mathbf{k} + \mathbf{p}) = \int \frac{d^3 \mathbf{p}'}{(2\pi)^3} \times \frac{1 - n_h^F(\mathbf{p} + \mathbf{p}' + \mathbf{k}) - n_h^F(-\mathbf{p}')}{\varepsilon + \varepsilon_h(\mathbf{k}) - \varepsilon_h(\mathbf{p} + \mathbf{p}' + \mathbf{k}) - \varepsilon_h(-\mathbf{p}')}$$

The analytic continuation for  $\Sigma_{hh}^{(2)}$  in the 2D case is similar to the one in the 3D case.

We note that for  $\Omega/T \gg 1$ , the bosonic distribution function  $n_B(\Omega) \rightarrow 0$  and the fermionic distribution function  $n_F(\Omega) \rightarrow \theta(\Omega)$  is the step-function. Hence at low temperatures  $\text{Im } \Sigma_{hh}$  and  $\text{Re } \Sigma_{hh}$  acquire the standard form [18, 19, 21]. In fact for low temperatures  $T \ll W_h \ll W_L$ , the most convenient way is to evaluate  $\text{Im } \Sigma_{hh}^{(2)}(\varepsilon)$  for  $T \rightarrow 0$ , which yields the standard Fermi-liquid result  $\text{Im } \Sigma_{hh}^{(2)}(\varepsilon) \sim \varepsilon^2$ , and then make the temperature averaging with the corresponding fermionic distribution function  $n_F(\varepsilon)$ . Therefore,  $\varepsilon \sim T$  for the scattering times of the quasiparticles. The evaluation of  $\Sigma_{hL}$ ,  $\Sigma_{Lh}$ , and  $\Sigma_{LL}$  at low temperatures in the first two orders in the gas parameter is similar to the evaluation of  $\Sigma_{hh}$  in both 3D and 2D cases.

But for higher temperatures, we should keep in mind that  $n_B(\Omega) \rightarrow T/\Omega$  for  $T \gg \Omega$ . The fermionic distribution function is “washed out” by temperature. Accordingly,  $n_F(\Omega) = (1 - \Omega/2T)/2$ . These approximations are important when we evaluate  $\text{Im } \Sigma$  for higher temperatures  $T > W_h$  [22].

We note that in contrast to the model of a slightly nonideal Fermi gas (see [18, 19, 21]), the Hubbard model does not contain an exchange-type diagram for  $\Sigma_{hh}$  (see Fig. 4) because the  $T$ -matrix in this diagram corresponds to the incoming and outgoing heavy particles with the same spin projection  $a_\sigma^+ a_\sigma^+ a_\sigma a_\sigma$ , while the Hubbard model contains only the matrix elements  $a_\uparrow^+ a_\downarrow^+ a_\downarrow a_\uparrow$ .

We also note that when we expand the  $T$ -matrix up to second order in the gas parameter, we implicitly assume that the  $T$ -matrix itself does not have a simple pole structure of the type of a bosonic propagator. This is the case for a partially filled band  $n_h d^D \ll 1$  and the low-energy sector where  $0 < \varepsilon < W_h \ll U_{hh}$ . Effectively, we neglect the lattice in this expansion.

However, taking the lattice into account produces two poles for the full (unexpanded)  $T$ -matrix of heavy particles in (15). The first one is connected with the so-called antibound state predicted by Hubbard [17] and Anderson [23] and corresponds to a large positive energy

$$\varepsilon \sim U_{hh} > 0. \tag{24}$$

Physically, it describes an antibound pair of two heavy particles with the energy  $U_{hh}$  on the same lattice site. It therefore reflects the presence of the upper Hubbard band already at low densities  $n_h d^D \ll 1$ . But the intensity of the upper Hubbard band is small at low densities and for the low-energy sector.

A second pole in the full  $T$ -matrix found by in [24] corresponds to a negative energy and in the 2D case yields

$$\varepsilon \approx -2\varepsilon_{Fh} - \frac{2\varepsilon_{Fh}^2}{W_h} < 0. \tag{25}$$

It describes the bound state of two holes below the bottom of the heavy band ( $\varepsilon < -2\varepsilon_{Fh}$ ). Therefore, it has zero imaginary part and does not contribute to  $\text{Im } T$ . (This mode produces nonanalytic corrections to  $\text{Re } \Sigma_{hh} \sim |\varepsilon|^{5/2}$  in 2D). We can neglect these two contributions for the self-energy when we calculate the effective masses and scattering times in the forthcoming sections. The more rigorous approach to the generalization of Galitskii results for the self-energy [18] to the case of finite temperatures (which is important for kinetic applications) will be a subject of a separate publication.

### 5. ELECTRON POLARON EFFECT

For  $T \rightarrow 0$ , the Green's functions for heavy and light electrons are given by

$$G_h(\omega, \mathbf{q}) = \frac{1}{\omega - \varepsilon_h(q) - \Sigma_h(\omega, \mathbf{q})} \approx \frac{Z_h}{\omega - \varepsilon_h^*(q) + i0}, \tag{26}$$

$$G_L(\omega, \mathbf{q}) \approx \frac{Z_L}{\omega - \varepsilon_L^*(q) + i0},$$

where

$$\varepsilon_h^*(q) = \frac{q^2 - p_{Fh}^2}{2m_h^*}, \quad \varepsilon_L^*(q) = \frac{q^2 - p_{FL}^2}{2m_L^*} \tag{27}$$

are renormalized quasiparticle spectra, and

$$Z_h^{-1} = \left( 1 - \frac{\partial \operatorname{Re} \Sigma_h^{(2)}(\omega, \mathbf{q})}{\partial \omega} \Big|_{\substack{\omega \rightarrow 0 \\ q \rightarrow p_{Fh}}} \right), \quad (28)$$

$$Z_L^{-1} = \left( 1 - \frac{\partial \operatorname{Re} \Sigma_L^{(2)}(\omega, \mathbf{q})}{\partial \omega} \Big|_{\substack{\omega \rightarrow 0 \\ q \rightarrow p_{FL}}} \right)$$

are  $Z$ -factors of heavy and light electrons. Substitution of the leading contribution from  $\operatorname{Re} \Sigma_{hL}^{(2)}(\omega, \mathbf{q})$  (described by a formula similar to (21)) to  $\operatorname{Re} \Sigma_h^{(2)}(\omega, \mathbf{q})$  in (28) yields

$$\lim_{\substack{\omega \rightarrow 0 \\ q \rightarrow p_{Fh}}} \frac{\partial \operatorname{Re} \Sigma_{hL}^{(2)}(\omega, \mathbf{q})}{\partial \omega} \sim - \left( \frac{4\pi a_{hL}}{m_{hL}^*} \right)^2 \iint \frac{d^D \mathbf{p}}{(2\pi)^D} \times$$

$$\times \frac{d^D \mathbf{p}'}{(2\pi)^D} \frac{[1 - n_L^F(\mathbf{p} + \mathbf{p}) - n_h^F(-\mathbf{p}')] n_L^F(\mathbf{p} - \mathbf{q})}{[\varepsilon_L(\mathbf{p} - \mathbf{q}) - \varepsilon_L(\mathbf{p}' + \mathbf{p}) - \varepsilon_h(-\mathbf{p}')]^2}, \quad (29)$$

where  $n_B(\Omega) \rightarrow 0$ ,  $n_F(\Omega)$  is a step function for  $\Omega/T \gg \gg 1$ ,  $a_{hL} \approx d$  in 3D is connected with the vacuum  $T$ -matrix  $T_{hL}$  and  $m_{hL}^* \approx m_L$ . Replacing

$$\frac{d^D \mathbf{p}}{(2\pi)^D} \frac{d^D \mathbf{p}'}{(2\pi)^D}$$

in (29) with  $N_L^2(0) d\varepsilon_L(\mathbf{p}) d\varepsilon_L(\mathbf{p}')$  (where  $N_L(0)$  is the density of states for light particles), and taking into account that  $\varepsilon_L(\mathbf{p} - \mathbf{q}) < 0$  while  $\varepsilon_L(\mathbf{p}' + \mathbf{p}) > 0$ , we can easily verify that for  $m_h \gg m_L$  (or equivalently for  $\varepsilon_{FL} \gg \varepsilon_{Fh}$ ) this expression contains a large logarithm (see [2]). Hence, the  $Z$ -factor of the heavy particles in the leading approximation is given by

$$Z_h^{-1} \approx 1 + 2f_0^2 \ln \frac{m_h}{m_L}, \quad (30)$$

where  $f_0 = 2p_{FL}d/\pi$  is the gas parameter in 3D and equivalently  $f_0 \approx 1/2 \ln(1/p_{FL}d)$  in 2D. We note that the contribution to  $Z_h$  from  $\operatorname{Re} \Sigma_{hh}^{(2)}$  does not contain a large logarithm. Correspondingly, for the effective mass of a heavy particle in (26), according to [19, 21], we obtain

$$\frac{m_h}{m_h^*} = Z_h \left( 1 + \frac{\partial \operatorname{Re} \Sigma_{hL}^{(2)}(\varepsilon_h(\mathbf{q}), \mathbf{q})}{\partial \varepsilon_h(\mathbf{q})} \Big|_{\varepsilon_h(q) \rightarrow 0} \right). \quad (31)$$

Therefore, as usual, the  $Z$ -factor contributes to the enhancement of the heavy mass:

$$\frac{m_h^*}{m_h} \sim Z_h^{-1} \sim \left( 1 + 2f_0^2 \ln \frac{m_h}{m_L} \right). \quad (32)$$

The analogous calculations for  $Z_L$  with  $\operatorname{Re} \Sigma_{Lh}$  and  $\operatorname{Re} \Sigma_{LL}$  yields only  $m_L^*/m_L \sim Z_L^{-1} \sim (1 + f_0^2)$ . If the

effective parameter  $2f_0^2 \ln(m_h/m_L) > 1$ , we are in the situation of a strong electron polaron effect. To obtain the correct polaron exponent in this region of parameters diagrammatically, we should at least sum up the so-called maximally crossed diagrams for  $\operatorname{Re} \Sigma_{hL}$ . But the exponent can also be evaluated in a different technique, based on the nonadiabatic part of the many-particle wave function [2] that describes a heavy particle dressed in a cloud of electron-hole pairs of light particles. This yields

$$\frac{m_h^*}{m_h} \sim Z_h^{-1} = \left( \frac{m_h}{m_L} \right)^{b/(1-b)}, \quad (33)$$

where  $b = 2f_0^2$ . For  $b = 1/2$  or, equivalently, for  $f_0 = = 1/2$  (as for the coupling constant of the screened Coulomb interaction in the RPA scheme), we are in the so-called unitary limit. In this limit, according to [2], the polaron exponent is

$$\frac{b}{1-b} = 1, \quad (34)$$

and hence

$$m_h^*/m_h = m_h/m_L \quad (35)$$

or, equivalently,

$$m_h^*/m_L = (m_h/m_L)^2. \quad (36)$$

Thus, starting from the ratio between the bare masses  $m_h/m_L \sim 10$  (obtained, for instance, in LDA approximation), we finish in the unitary limit with  $m_h^*/m_L \sim \sim 100$  (due to the many-body EPE), which is a typical ratio for uranium-based heavy-fermion (HF) systems.

### 5.1. Other mechanisms of heavy mass enhancement

We note that rigorously speaking (see (31)), the momentum dependence of  $\operatorname{Re} \Sigma_{hL}^{(2)}(\varepsilon_h(\mathbf{q}), \mathbf{q})$  is also very important for the evaluation of the effective mass. Very preliminary estimates by Prokof'ev and a present authors show that in the zeroth approximation in  $m_L/m_h$ , in the 3D case close to the Fermi surface (for  $\varepsilon_h(q) = (q^2 - p_{Fh}^2)/2m_h \rightarrow 0$  and  $q \rightarrow p_{Fh}$ ),

$$\operatorname{Re} \Sigma_{hL}^{(2)}(\varepsilon_h(\mathbf{q}), \mathbf{q}) \approx 2 \left( \frac{4\pi a_{hL}}{m_L} \right)^2 \times$$

$$\times \int \frac{d^3 \mathbf{p}}{(2\pi)^3} \Pi_{LL}(0, \mathbf{p}) n_h^F(\mathbf{p} - \mathbf{q}), \quad (37)$$

where

$$\Pi_{LL}(0, \mathbf{p}) = \int \frac{d^3 \mathbf{p}'}{(2\pi)^3} \frac{n_L^F(\varepsilon_{p'+p}) - n_L^F(\varepsilon_{p'})}{\varepsilon_L(\mathbf{p}') - \varepsilon_L(\mathbf{p}' + \mathbf{p})} \quad (38)$$

is the static polarization operator for light particles. Having in mind that  $|\mathbf{p}-\mathbf{q}| < p_{Fh}$  and  $q \approx p_{Fh}$  in (37), we can see that  $\mathbf{p} \rightarrow 0$  and use the asymptotic form for  $\Pi_{LL}(0, \mathbf{p})$  at small  $p \ll p_{FL}$  (if the densities of heavy and light bands are not very different and  $p_{FL} \sim p_{Fh}$ ):

$$\lim_{p \rightarrow 0} \Pi_{LL}(0, \mathbf{p}) = N_L(0) \left( 1 - \frac{p^2}{12p_{FL}^2} \right), \quad (39)$$

where  $N_L(0) = m_L p_{FL} / 2\pi^2$  is the density of states for light electrons in 3D. The substitution of  $\lim_{p \rightarrow 0} \Pi_{LL}(0, \mathbf{p})$  from (39) in (37) yields

$$\begin{aligned} \text{Re } \Sigma_{hL}^{(2)}(\varepsilon_h(\mathbf{q}), \mathbf{q}) &\approx \text{Re } \Sigma_{hL}^{(2)}(0, p_{Fh}) - \\ &- \frac{(q^2 - p_{Fh}^2)}{2m_h} \frac{f_0^2}{9} \frac{m_h n_h}{m_L n_L}, \end{aligned} \quad (40)$$

where  $f_0 \approx 2dp_{FL}/\pi$  is the 3D gas parameter and  $n_h = p_{Fh}^3/3\pi^2$  and  $n_L = p_{FL}^3/3\pi^2$  are the densities of heavy and light bands.

The first term in (40) describes  $\text{Re } \Sigma_{hL}^{(2)}(\varepsilon_h(\mathbf{q}), \mathbf{q})$  on the Fermi surface (for  $\varepsilon_h(q) = 0$  and  $q = p_{Fh}$ ):

$$\begin{aligned} \text{Re } \Sigma_{hL}^{(2)}(0, p_{Fh}) &\approx \frac{4f_0^2}{3} \frac{n_h}{n_L} \times \\ &\times \varepsilon_{FL} \left( 1 - \frac{2p_{Fh}^2}{15p_{FL}^2} \right) > 0 \quad \text{for } p_{Fh} \sim p_{FL}. \end{aligned} \quad (41)$$

It is a renormalization of the effective chemical potential of the heavy band in the second order in the gas parameter due to the interaction of light and heavy particles.

We note that according to [18, 19], the renormalized heavy-particle spectrum is given by

$$\begin{aligned} \varepsilon_h^*(q) &= \left( \frac{q^2}{2m_h} - \mu_h^{eff} \right) + \frac{2\pi}{m_L} n_L(\mu) a_{hL} + \\ &+ \text{Re } \Sigma_{hL}^{(2)}(\varepsilon_h(\mathbf{q}), \mathbf{q}) = \frac{q^2 - p_{Fh}^2}{2m_h^*}, \end{aligned} \quad (42)$$

where the scattering length  $a_{hL} \approx d$ , the effective chemical potential  $\mu_h^{eff} = \mu_h + W_h/2 + \varepsilon_0$  is counted from the bottom of the heavy band, and the Hartree–Fock term  $(2\pi/m_L)n_L(\mu) a_{hL}$  represents the contribution to the self-energy  $\text{Re } \Sigma_{hL}^{(1)}$  in the first order in the gas parameter. From (42), collecting the terms proportional to  $\varepsilon_h(q) = (q^2 - p_{Fh}^2)/2m_h$ , we obtain

$$\frac{q^2 - p_{Fh}^2}{2m_h^*} = \varepsilon_h(q) \left( 1 - \frac{f_0^2}{9} \frac{m_h n_h}{m_L n_L} \right). \quad (43)$$

Correspondingly, the effective mass of a heavy particle is given by

$$\begin{aligned} \frac{m_h}{m_h^*} &= \left( 1 + \frac{\partial \text{Re } \Sigma_{hL}^{(2)}(\varepsilon_h(\mathbf{q}), \mathbf{q})}{\partial \varepsilon_h(q)} \Big|_{\varepsilon_h \rightarrow 0} \right) = \\ &= 1 - \frac{f_0^2}{9} \frac{m_h n_h}{m_L n_L}. \end{aligned} \quad (44)$$

As a result, we obtain a much more dramatic enhancement of  $m_h^*$  than in the EPE, which yields only  $m_h/m_h^* \approx (1 - 2f_0^2 \ln(m_h/m_L))$  due to the  $Z$ -factor of a heavy particle. For  $m_h/m_L \sim 10$ , the contribution to  $m_h^*$  in (44) becomes larger than the contribution from the  $Z$ -factor in (32) for a large density mismatch  $n_h \geq 5n_L$  between the heavy and light bands. We note that the contribution to  $m_h^*/m_h$  from  $\text{Re } \Sigma_{hh}^{(2)}(\varepsilon_h(\mathbf{q}), \mathbf{q})$  associated with the “heavy–heavy” interaction is small in comparison with the contribution to  $m_h^*$  from  $\text{Re } \Sigma_{hL}^{(2)}$  (which is associated with the “heavy–light” interaction) due to the smallness of the ratio between the bare masses:  $m_L/m_h \ll 1$ . We can now collect the terms that do not depend on  $\varepsilon_h(q)$  in (42). This gives the effective chemical potential of heavy electrons

$$\mu_h^{eff} = \frac{p_{Fh}^2}{2m_h} + \frac{2\pi}{m_L} n_L(\mu) a_{hL} + \text{Re } \Sigma_{hL}^{(2)}(0, p_{Fh}). \quad (45)$$

We note that the contributions to  $\mu_h^{eff}$  from the Hartree–Fock term  $(2\pi/m_h)n_h(\mu) a_{hh}$  of heavy electrons and from  $\text{Re } \Sigma_{hh}^{(2)}(0, p_{Fh})$  (which is connected with “heavy–heavy” interactions) are small in comparison with “heavy–light” contributions due to the smallness of the ratio between the bare masses:  $m_L/m_h \ll 1$ .

In 2D, the static polarization operator is

$$\Pi_{LL}(0, \mathbf{p}) = \frac{m_L}{2\pi} \left( 1 - \text{Re } \sqrt{1 - \frac{4p_{FL}^2}{p^2}} \right),$$

and hence for  $p < 2p_{FL}$ ,  $\Pi_{LL}(0, \mathbf{p}) = m_L/2\pi$  does not contain any dependence on  $p^2$ , in contrast to the 3D case. Thus, the EPE in 2D is a dominant mechanism of the heavy mass enhancement.

A more accurate evaluation of the momentum dependence of  $\text{Re } \Sigma_{hL}^{(2)}(\varepsilon_h(\mathbf{q}), \mathbf{q})$  for the larger densities in the bands together with the summation of the higher-order contributions to  $\text{Re } \Sigma_{hL}$  will be a subject of a separate investigation.

We note that for the light particles, the momentum dependences of  $\text{Re } \Sigma_{Lh}^{(2)}$  and  $\text{Re } \Sigma_{LL}^{(2)}$  yield only  $m_L^*/m_L \sim 1 + f_0^2$ , and hence the light mass is not strongly enhanced in both 3D and 2D cases.

## 5.2. The tendency towards phase separation

We also note that for larger densities of the heavy band  $n_h \sim n_C \leq 1$  (and large difference in densi-

ties between the bands,  $n_L \ll n_h$ , whence  $n_{tot}d^D = (n_h + n_L)d^D \leq 1$ , another mechanisms of heavy mass enhancement become more effective. Namely, for these densities and a large mismatch between  $n_h$  and  $n_L$ , we could have a tendency towards phase separation in a two-band model [14].

We note that if we analyze the effective chemical potential of the heavy band in (45) in the limit of the large density mismatch  $n_h \gg n_L$  in 3D and evaluate the partial compressibility (the sound velocity of heavy particles squared)

$$\kappa_{hh}^{-1} \sim c_h^2 = \frac{n_h}{m_h} \frac{\partial \mu_h}{\partial n_h},$$

we already see the tendency towards phase separation (towards negative compressibility) in the strong-coupling limit and low densities for  $f_0^2 m_h p_{Fh} / m_L p_{FL} \gtrsim 1$ , in qualitative agreement with the results in [14]. A more careful analysis of all the partial compressibilities in the system at larger  $f_0$  and a large mismatch between the densities will be reported elsewhere.

In the end of this section, we emphasize that the physics of the EPE and evaluation of  $Z_h$  in [2] are to some extent connected with the well-known results of Nozieres et al. [25] on infrared divergences in the description of the Brownian motion of a heavy particle in a Fermi liquid and on the infrared divergences for the problem of X-ray photoemission from the deep electron levels, as well as with the famous results of Anderson [26] on the orthogonality catastrophe for the 1D chain of  $N$  electrons under the addition of one impurity to the system.

Finally, we mention a competing mechanism proposed in [27] first for an explanation of the effective mass in praseodymium (Pr) and in some uranium-based molecules like  $U(C_8H_8)_2$ . Later on, Fulde et al. [27] generalized this mechanism to some other uranium-based HF-compounds with localized and delocalized orbitals. This mechanism has a quantum chemical nature and is based on the scattering of conductive electrons on localized orbitals as if on two-level systems. The mass enhancement is here governed by non-diagonal matrix elements of the Coulomb interaction, which are not contained in the simple version of a two-band model in (1). In this context, we also mention [28], where the authors considered the mass enhancement of conductivity electrons due to their scattering on local  $f$ -levels splitted by the crystalline field.

We note that dHvA experiments [29] together with ARPES experiments [30] and thermodynamic measurements [31] are the main instruments to reconstruct the Fermi surface for HF compounds and to deter-

mine the effective mass (thus verifying the predictions of different theories regarding the mass enhancement in uranium-based HF compounds).

## 6. TEMPERATURE DEPENDENCE OF THE RESISTIVITY

### 6.1. Imaginary parts of self-energies in the homogeneous case for low temperatures $T < W_h$

In the homogeneous case, after averaging  $\text{Im} \Sigma^{(2)}(\varepsilon(\mathbf{q}), \mathbf{q})$  in (20) with the fermionic distribution function  $n_F(\varepsilon(\mathbf{q})/T)$ , we obtain the following expression for  $\text{Im} \Sigma^{(2)}(T)$  of heavy and light electrons at low temperatures  $T \ll W_h$  and for equal densities  $n_h = n_L$  in the heavy and light bands:

$$\begin{aligned} \text{Im} \Sigma_{LL}^{(2)}(T) &= f_0^2 \frac{T^2}{\varepsilon_{FL}}, \\ \text{Im} \Sigma_{Lh}^{(2)}(T) &= f_0^2 \frac{T^2}{\varepsilon_{Fh}} \frac{m_h}{m_L} \end{aligned} \quad (46)$$

and accordingly:

$$\text{Im} \Sigma_{hh}^{(2)}(T) = f_0^2 \frac{T^2}{\varepsilon_{Fh}}, \quad \text{Im} \Sigma_{hL}^{(2)}(T) = f_0^2 \frac{T^2}{\varepsilon_{Fh}}. \quad (47)$$

It follows that all  $\text{Im} \Sigma^{(2)}(T)$  behave in the standard Fermi-liquid fashion  $\text{Im} \Sigma^{(2)}(T) \sim T^2$ .

Moreover,  $\text{Im} \Sigma_{Lh}^{(2)}(T) \gg \text{Im} \Sigma_{LL}^{(2)}(T)$ , and hence

$$\begin{aligned} \text{Im} \Sigma_L^{(2)}(T) &= \text{Im} \Sigma_{Lh}^{(2)}(T) + \text{Im} \Sigma_{LL}^{(2)}(T) \approx \\ &\approx \text{Im} \Sigma_{Lh}^{(2)}(T). \end{aligned} \quad (48)$$

We can now estimate the Drude conductivity for the light band:

$$\sigma_L = \frac{n_L e^2 \tau_L}{m_L}, \quad (49)$$

where a naive estimate for  $\tau_L$  yields

$$\gamma_L = 1/\tau_L = \text{Im} \Sigma_L^{(2)}(T) = \text{Im} \Sigma_{Lh}^{(2)}(T), \quad (50)$$

whence  $1/\tau_L \approx 1/\tau_{Lh}$ . Correspondingly, we obtain the conductivity

$$\begin{aligned} \sigma_L \approx \sigma_{Lh} &= \frac{n_L e^2 \tau_{Lh}}{m_L} = \frac{n_L e^2}{f_0^2 T^2} \frac{\varepsilon_{Fh} m_L}{m_h m_L} = \\ &= \frac{n_L e^2}{f_0^2 p_{Fh}^2} \left( \frac{\varepsilon_{Fh}}{T} \right)^2. \end{aligned} \quad (51)$$

Introducing the minimal Mott–Regel conductivities

$$\begin{aligned} \sigma_{min} &= \left( \frac{e^2}{\hbar} \right) p_F \quad \text{in 3D} \\ \text{and } \sigma_{min} &= \left( \frac{e^2}{\hbar} \right) \quad \text{in 2D} \end{aligned} \quad (52)$$

and working in the units where  $\hbar = 1$ , in the case of equal densities of heavy and light bands,  $n_h = n_L$ , we obtain

$$\sigma_L \approx \sigma_{Lh} = \frac{\sigma_{min}}{f_0^2} \left( \frac{\varepsilon_{Fh}}{T} \right)^2. \quad (53)$$

We note that, strictly speaking, the nondiagonal conductivity  $\sigma_{Lh}$  (which is defined by the scattering of light electrons on the heavy ones) is finite only due to an account of umklapp processes:

$$\mathbf{p}_{1L} + \mathbf{p}_{2h} = \mathbf{p}_{3L} + \mathbf{p}_{4h} + \mathbf{K}, \quad (54)$$

where  $K \sim \pi/d$  is the wave vector of the reciprocal lattice. For  $p_{Fh} \sim p_{FL}$ , this means that densities in the light and heavy bands cannot be very small (otherwise the conductivity  $\sigma_{Lh}$  would be exponentially large). Hence, within the accuracy of our estimates,

$$\sigma_{Lh} = \frac{\sigma_{min}}{f_0^2} \left( \frac{W_h}{T} \right)^2. \quad (55)$$

The situation with the conductivity of the heavy band is a slightly more tricky since  $\text{Im} \Sigma_{hh}^{(2)}(T) \sim \text{Im} \Sigma_{hL}^{(2)}(T)$  and hence  $\sigma_{hh} \sim \sigma_{hL}$ . However, for a crude estimate, we can again consider only the nondiagonal part of the conductivity  $\sigma_{hL}$  and take umklapp processes (54) into account. Then

$$\sigma_{hL} \sim \sigma_{Lh} \sim \frac{\sigma_{min}}{f_0^2} \left( \frac{W_h}{T} \right)^2. \quad (56)$$

We note that estimates (56) for  $\sigma_{Lh}$  and  $\sigma_{hL}$  can be verified using the exact solution of coupled kinetic equations for heavy and light particles with an account of umklapp processes [22].

The total resistivity is given by

$$R = \frac{1}{\sigma_h + \sigma_L} \sim \frac{f_0^2}{\sigma_{min}} \left( \frac{T}{W_h} \right)^2. \quad (57)$$

It behaves in a Fermi-liquid manner  $R(T) \sim T^2$  for low temperatures  $T < W_h$ . For  $m_h^* \gg m_h$ , we can replace  $W_h$  with  $W_h^*$  in (56) and (57).

### 6.2. The chemical potential at higher temperatures $T > W_h^*$

If  $T > W_h^*$ , the heavy band is totally destroyed (more precisely, it is destroyed for  $f_0^2 T = W_h^*$  as we see shortly). To be accurate, we first calculate the effective chemical potential  $\mu_h^{eff} = \mu + W_h/2 + \varepsilon_0$  in (3) in this situation.

Generally speaking,  $n_h + n_L = n_{tot} = \text{const}$ , i.e., only the total density is conserved. In our case,

however, for large difference between the bare masses  $m_h \gg m_L$ , each density of the band is conserved practically independently,  $n_h \approx \text{const}$  and  $n_L \approx \text{const}$ . For heavy particles, all the states in the band are uniformly occupied at these temperatures. For  $T > W_h$  (assuming  $m_h^*/m_h \sim 1$ ), the effective chemical potential of the heavy particles is given by

$$\mu_h^{eff} = \mu + \frac{W_h}{2} + \varepsilon_0 \sim -T \ln \left( \frac{1}{n_h d^D} \right). \quad (58)$$

Hence, we have the Boltzman behavior for  $\mu_h^{eff}$ . The Fermi–Dirac distribution function for heavy particles is

$$\begin{aligned} n_h(\varepsilon) &= \frac{1}{\exp \left( \frac{p^2 \cdot 2m_h - \mu_h^{eff}}{T} \right) + 1} \approx \\ &\approx \frac{1}{\left( 1 + \frac{p^2}{2m_h T} \right) \exp \left( -\frac{\mu_h^{eff}}{T} \right) + 1} \approx \\ &\approx \frac{\exp(\mu_h^{eff}/T)}{1 + \frac{p^2}{2m_h T}} \approx \exp \left( \frac{\mu_h^{eff}}{T} \right) = \text{const}. \end{aligned} \quad (59)$$

For light particles for the temperatures  $W_h \ll T \ll W_L$ , because  $m_h \gg m_L$ , the effective chemical potential has approximately the same position as for  $T = 0$ . Indeed, for  $\mu_{eff}^L = \mu + W_L/2$  we have

$$\begin{aligned} n_L(\varepsilon) &= \frac{1}{\exp \left( \frac{p^2 \cdot 2m_L - \mu_h^{eff}}{T} \right) + 1} \approx \\ &\approx \frac{1}{\exp \left( \frac{p^2 - p_{FL}^2}{2m_L T} \right) + 1} \approx \\ &\approx \theta \left( \frac{p^2}{2m_L} - \varepsilon_{FL} \right), \quad T \ll \varepsilon_{FL}, \end{aligned} \quad (60)$$

and hence the effective chemical potential of light particles is

$$\mu_{eff}^L \approx \varepsilon_{FL}. \quad (61)$$

### 6.3. Evaluation of the imaginary parts of the self-energies at higher temperatures $W_h^* < T < W_L$

For light particles,  $\text{Im} \Sigma_{LL}^{(2)}(T) = f_0^2 T^2 / W_L$  does not change. But

$$\text{Im} \Sigma_{Lh}^{(2)}(T) = f_0^2 W_h \frac{m_h}{m_L} \gg \text{Im} \Sigma_{LL}^{(2)}(T) \quad (62)$$

for  $W_h^* < T < W_L$  (for  $T < W_L$ ,  $T^2/W_L < W_h m_h/m_L$ ).

This describes almost elastic scattering of light electrons on the heavy ones as if on immobile (static) impurities in the zeroth order in  $W_h/W_L$ . We note that  $W_h m_h = W_h^* m_h^*$ . For heavy electrons, we should account for the bosonic contribution  $n_B(\Omega) \approx T/\Omega$  and the fermionic contribution  $n_F(\Omega) \approx (1 - \Omega/2T)/2$  for  $\Omega/T \ll 1$  to  $\text{Im } \Sigma^{(2)}$  and thus to scattering times. This yields

$$\text{Im } \Sigma_{hh}^{(2)}(T) = f_0^2 W_h, \quad (63)$$

which describes scattering of heavy electrons on each other in the situation when they uniformly occupy the heavy band and can transfer to each other only an energy  $\sim W_h$  [2]. Because  $m_h^* \gg m_h$ , we can replace  $W_h$  with  $W_h^*$  in (63). At the same time, for scattering of heavy particles on the light ones, we have

$$\text{Im } \Sigma_{hL}^{(2)}(T) = f_0^2 T \gg \text{Im } \Sigma_{hh}^{(2)}(T), \quad (64)$$

which describes the marginal Fermi-liquid behavior for diffusive motion of heavy electrons in the surrounding of light electrons.

We note that to derive (64) for  $W_L > T > W_h$  and in the zeroth order in the mass ratio  $m_L/m_h \ll 1$ , we rewrote expression (20) for  $\text{Im } \Sigma_{hL}^{(2)}(\varepsilon_h(\mathbf{p}), \mathbf{p})$  in the form

$$\begin{aligned} \text{Im } \Sigma_{hL}^{(2)}(\varepsilon_h(\mathbf{p}), \mathbf{p}) &= -\pi \left( \frac{4\pi a_{hL}}{m_L} \right)^2 N_L^2(0) \times \\ &\times \iint d\varepsilon_{Lp'} d\varepsilon_{Lk} \delta(\varepsilon_{Lk} - \varepsilon_{Lp'}) n_F(\varepsilon_{Lk}) \times \\ &\times [1 - n_F(\varepsilon_{Lp'})], \end{aligned} \quad (65)$$

which after the  $\delta$ -function integration yielded

$$\begin{aligned} \text{Im } \Sigma_{hL}^{(2)}(\varepsilon_h(\mathbf{p}), \mathbf{p}) &\sim \pi f_0^2 \int d\varepsilon_{Lk} n_F(\varepsilon_{Lk}) \times \\ &\times [1 - n_F(\varepsilon_{Lk})] \sim \\ &\sim \pi f_0^2 \int_{-\infty}^{\infty} d\varepsilon \frac{e^{\varepsilon/T}}{(1 + e^{\varepsilon/T})^2} \sim f_0^2 T. \end{aligned} \quad (66)$$

#### 6.4. Resistivity for $T > W_h^*$ in the 3D case

From the previous section, we have the scattering times of heavy and light particles for  $T > W_h^*$  given by

$$\frac{1}{\tau_L} \approx \frac{1}{\tau_{Lh}} = f_0^2 W_h \frac{m_h}{m_L}. \quad (67)$$

We note that  $f_0^2 W_h m_h/m_L = f_0^2 W_h^* m_h^*/m_L \sim f_0^2 W_L$  in (67). In the same time,

$$\frac{1}{\tau_h} \approx \frac{1}{\tau_{hh}} = f_0^2 T, \quad (68)$$

and hence the heavy component is marginal, but the light one is not. The light band conductivity is given by

$$\sigma_L = \frac{n_L e^2 \tau_L}{m_L} \approx \frac{n_L e^2 \tau_{Lh}}{m_L} = \frac{\sigma_{min}}{f_0^2}. \quad (69)$$

For the heavy band, the Drude formula must be modified  $\partial n_h/\partial T \sim W_h^*/T$  because of  $T > W_h^*$ . We then immediately obtain

$$\sigma_h = \frac{\sigma_{min}}{f_0^2} \left( \frac{W_h^*}{T} \right)^2. \quad (70)$$

As a result, the resistivity is

$$\begin{aligned} R &= \frac{1}{\sigma_h + \sigma_L} = \frac{f_0^2}{\sigma_{min}} \frac{(T/W_h^*)^2}{1 + (T/W_h^*)^2} = \\ &= \frac{f_0^2}{\sigma_{min}} \frac{1}{1 + (W_h^*/T)^2}. \end{aligned} \quad (71)$$

For  $T > W_h^*$ , the resistivity  $R \approx f_0^2/\sigma_{min}$  saturates. We thus obtain a residual resistivity at high temperatures due to the conductivity of the light band. This is a very nontrivial result.

#### 6.5. Discussion of the obtained results for resistivity at higher temperatures

When  $W_h^* < 1/\tau_h$  or, equivalently,  $f_0^2 T > W_h^*$ , the coherent motion in the heavy band is totally destroyed. The heavy particles begin to move diffusively in the surrounding of light particles. In this regime, rigorously speaking, the diagram technique can be used only for light particles and not for heavy ones.

But the exact solution of the density matrix equation obtained in [2] shows that  $1/\tau_{hL}$  is qualitatively the same for  $f_0^2 T > W_h^*$  as in our estimates, and the inverse scattering time  $1/\tau_{Lh}$  is also qualitatively the same due to its physical meaning (scattering of light electrons on heavy ones as if on immobile impurities). That is why  $\sigma_h$  and  $\sigma_L$  and hence  $R(T)$  behave smoothly for  $f_0^2 T \geq W_h^*$ .

#### 6.6. An idea of a hidden heavy band for HTSC

The resistivity  $R(T)$  in 3D acquires a form (see Fig. 5) that is frequently obtained in uranium-based HF (for example,  $\text{UNi}_2\text{Al}_3$ ). We note that  $R(T)$  mimics a linear behavior in the crossover region of intermediate temperatures  $T \sim W_h^*$  between  $T^2$  and const (with the resistivity saturating for  $T \gg W_h^*$ ). The same holds

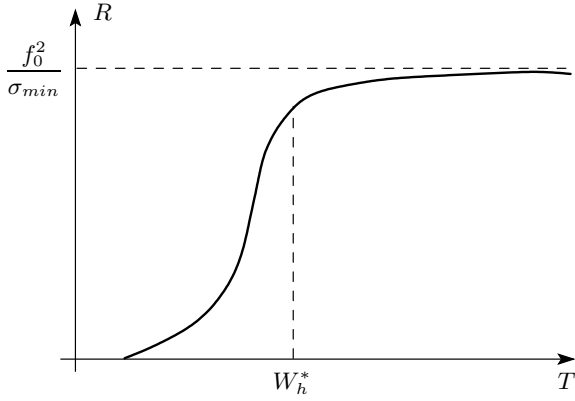


Fig. 5. The resistivity  $R(T)$  in the two-band model in 3D

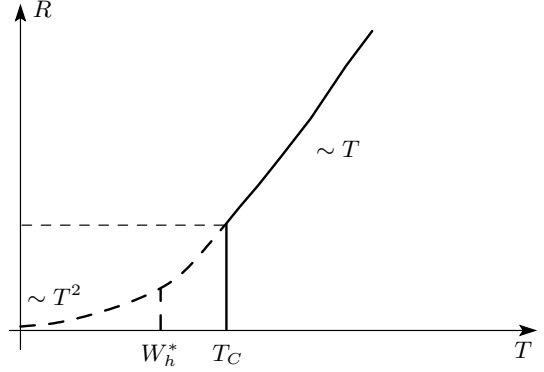


Fig. 6. Resistivity  $R(T)$  in a superconducting material with a hidden heavy band for  $W_h^* < T_C$  ( $W_h^*$  is an effective width of the heavy band)

for magnetoresistance in the well-known experiments of P. L. Kapitza,

$$\frac{R(H) - R(0)}{R(H)} \sim \frac{(\Omega_C \tau)^2}{1 + (\Omega_C \tau)^2} \sim \begin{cases} (\Omega_C \tau)^2, & \Omega_C \tau < 1, \\ \text{const}, & \Omega_C \tau > 1, \end{cases} \quad (72)$$

where  $\Omega_C$  is the cyclotron frequency.

In the crossover region  $\Omega_C \tau \sim 1$ , the magnetoresistance mimics a behavior linear in  $\Omega_C$ . It then follows that for  $T > W_h^*$ , heavy electrons are marginal, but light electrons are not. The natural question arises whether it is possible to make light electrons also marginal and as a result to obtain the resistivity such that  $R(T) \sim T$  is marginal for  $T > W_h^*$ , but  $R(T) \sim T^2$  for  $T < W_h^*$ . Such resistivity characteristics could serve as an alternative scenario for the explanation of the normal properties in optimally doped or slightly overdoped HTSC materials if we assume the existence of a hidden heavy band with a bandwidth smaller than the superconductive critical temperature  $T_C$ :  $W_h^* < T_C$  (see Fig. 6). To obtain the Fermi-liquid behavior  $R(T) \sim T^2$  at low temperatures, we should then suppress SC by a large magnetic field  $H$  to low critical temperatures  $T_C(H) < W_h^*$ .

### 7. WEAK-LOCALIZATION CORRECTIONS IN THE 2D CASE

The tendency towards marginalization of the light component manifests itself in the 2D case. We know that logarithmic corrections [3] to the classical Drude formula for conductivity occur in 2D due to weak localization effects. But according to our ideology, heavy

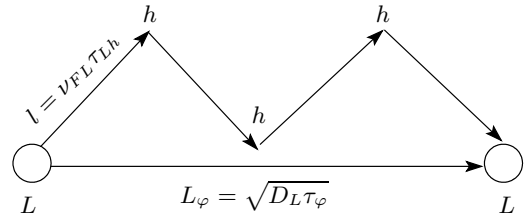


Fig. 7. Multiple scattering of a light particle on heavy ones in the interval between the scattering of the light particle on another light particles.  $L_\varphi$  is the diffusive length,  $l$  is the elastic length,  $D_L$  and  $v_{FL}$  are the diffusion coefficient and the Fermi velocity for light electrons, and  $\tau_{Lh}$  and  $\tau_\varphi$  are the elastic time for scattering of light electrons on heavy ones and the inelastic (decoherence) time

particles play the role of impurities for scattering of light particles on them. That is why the correct expression for the conductivity of the light band  $\sigma_L$  in the absence of spin-orbital coupling is given by

$$\sigma_L^{loc} = \frac{\sigma_{min}}{f_0^2} \left( 1 - f_0^2 \ln \frac{\tau_\varphi}{\tau} \right), \quad (73)$$

where, according to the weak localization theory in 2D,  $\tau$  is the elastic time and  $\tau_\varphi$  is the inelastic (decoherence) time. In our case,

$$\tau = \tau_{ei} = \tau_{Lh}, \quad \text{while} \quad \tau_\varphi = \tau_{ee} = \tau_{LL}, \quad \text{and} \quad \tau_{LL} \gg \tau_{Lh}, \quad (74)$$

where  $\tau_{ei}$  and  $\tau_{ee}$  are the times associated with the scattering of electrons on impurities and other electrons, respectively. Hence, between two scatterings of a light particle on another light one, it scatters on heavy particles many times (see Fig. 7). As a result, the motion

of light particles becomes much slower (also of the diffusive type) and two characteristic lengths appear in the theory: the elastic length

$$l = v_{FL} \tau_{Lh} \quad (75)$$

and the diffusive length

$$L_\varphi = \sqrt{D_L \tau_\varphi}, \quad (76)$$

where  $D_L$  is the diffusion coefficient for light electrons and  $v_{FL}$  is the Fermi velocity for light electrons.

That is why in a more rigorous theory, according to [3] we should replace the inverse scattering time

$$\frac{1}{\tau_{LL}(\varepsilon)} \sim \int_0^\varepsilon d\omega \int_0^\omega d\varepsilon' \int_0^\infty \frac{a_{LL}^2}{m_L^2} \frac{q dq}{(v_{FL} q)^2} = f_0^2 \frac{T^2}{W_L} \quad (77)$$

with

$$\frac{1}{\tilde{\tau}_{LL}(\varepsilon)} \sim \int_0^\varepsilon d\omega \int_0^\omega d\varepsilon' \int_0^\infty \frac{a_{LL}^2}{m_L^2} \frac{q dq}{(i\varepsilon' + D_L q^2)^2}, \quad (78)$$

where the scattering length  $a_{LL} \sim d$ . In fact, we replace  $v_{FL} q$  with the ‘‘cooperon’’ pole  $(i\varepsilon' + D_L q^2)$  in Altshuler–Aronov terminology. Hence, the characteristic wave vectors in the evaluation of  $\tilde{\tau}_{LL}$  are  $q \sim \sqrt{\varepsilon/D_L}$ , where  $\varepsilon$  is an energy variable. The Altshuler–Aronov effect in 2D yields

$$\frac{1}{\tilde{\tau}_{LL}(\varepsilon)} = f_0^2 \frac{\varepsilon}{N_L(0) D_L}, \quad (79)$$

where  $N_L(0) = m_L/2\pi$  is the 2D density of states for light electrons. For the diffusion coefficient, we can use the estimate

$$D_L = v_{FL}^2 \tau_{Lh} \quad (80)$$

and hence, having in mind that according to (68) the inverse scattering time is  $1/\tau_{Lh}(\varepsilon) = f_0^2 W_h m_h/m_L \approx f_0^2 W_L$ , we obtain

$$\frac{1}{\tilde{\tau}_{LL}(\varepsilon)} \sim \frac{f_0^2 f_0^2 W_L}{m_L v_{FL}^2 / \pi} \varepsilon \sim f_0^4 \varepsilon. \quad (81)$$

Therefore,  $1/\tilde{\tau}_{LL}$  also becomes marginal for  $\varepsilon \sim T$ . For logarithmic corrections to the conductivity, we have

$$\frac{\tau_\varphi}{\tau} = \frac{\tilde{\tau}_{LL}}{\tau_{Lh}} = \frac{W_L}{f_0^2 T} \gg 1, \quad (82)$$

and hence

$$\sigma_L^{loc} = \frac{\sigma_{min}}{f_0^2} \left( 1 - f_0^2 \ln \frac{W_L}{f_0^2 T} \right). \quad (83)$$

For  $f_0^2 T \sim W_h$ ,  $\ln(W_L/f_0^2 T) \sim \ln(W_L/W_h)$  and

$$Z_h = \frac{\sigma_L^{loc}}{\sigma_L} = 1 - f_0^2 \ln \frac{W_L}{W_h}. \quad (84)$$

Therefore, for  $f_0^2 T \sim W_h$ , an enhancement of the heavy-particle  $Z$ -factor due to the EPE and localization of light particles due to Altshuler–Aronov corrections are governed by the same parameter  $f_0^2 \ln(m_h/m_L)$  in 2D.

### 7.1. Justification of the expression for localization corrections in 2D

In principle, the impurities (heavy particles) are mobile and have some recoil energy. That is why the formula  $\sigma_L^{loc}/\sigma_L = 1 - f_0^2 \ln(W_L/f_0^2 T)$  should be justified (at least as regards the temperature exponent under logarithm,  $T$  or  $T^\alpha$ ). For the justification, we need to estimate the loss of energy by one light particle before it collides with another light particle. The number of collisions with heavy particles between the scattering of a light particle on light one is  $L_\varphi/l$ . The maximal loss of energy in one collision is  $W_h^*$ . The total loss is  $W_h^* L_\varphi/l = W_h^* \sqrt{W_L/T}$ . The energy of light particle itself is  $T$ . This means that for  $W_h^* \sqrt{W_L/T} < T$  or, equivalently, for

$$T > W_h^* \left( \frac{W_L}{f_0^2 W_h^*} \right)^{1/3}, \quad (85)$$

the loss of energy is small and heavy particles can be regarded as immobile impurities. Hence, the exponent  $\alpha$  under the logarithm is 1.

### 7.2. Resistivity in the 2D case

Qualitatively, the resistivity behaves in 2D as

$$R = \frac{f_0^2}{\sigma_{min}} \frac{1}{(W_h^*/T)^2 + 1 - f_0^2 \ln(W_L/f_0^2 T)}. \quad (86)$$

It has a maximum at  $T_{max} \sim W_h^*/f_0$  and a localization tail at higher temperatures (see Fig. 8). It would be very interesting to find the magnetoresistance in the 2D or layered case in a two-band model with one narrow band for a strong quantizing magnetic field  $H$  oriented perpendicular to the layers [33].

## 8. SUPERCONDUCTIVITY IN THE TWO-BAND MODEL WITH ONE NARROW BAND

In the end of this paper, we mention briefly that the leading SC mechanism at the low electron density corresponds to  $p$ -wave pairing and is governed, especially

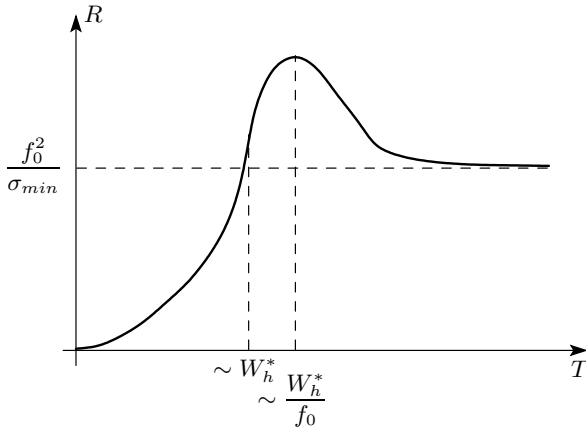


**Fig. 8.** Resistivity  $R(T)$  in the 2D case for the two-band model with one narrow band. The resistivity exhibits a maximum and a localization tail at higher temperatures  $T > W_h^*$

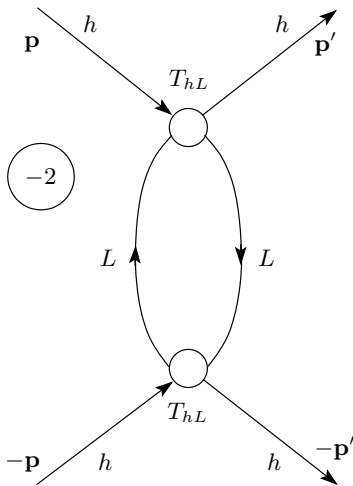


**Fig. 9.** The leading contribution to the effective interaction  $V_{eff}$  for the  $p$ -wave pairing of heavy particles via polarization of light particles. The open circles stand for the vacuum  $T$ -matrix  $T_{hL}$

in 2D, by the pairing of heavy electrons via polarization of light ones (see Fig. 9 and [15, 16]) in the framework of enhanced Kohn–Luttinger mechanism [4]. The corresponding  $T_c$  depends on the relative doping of the bands  $n_h/n_L$  nonmonotonically and has a broad and pronounced maximum for  $n_h/n_L = 4$  in 2D, where it could reach the experimentally feasible values realistic for layered ruthenates  $\text{Sr}_2\text{RuO}_4$  [39] and uranium-based heavy-fermion compounds like  $\text{U}_{1-x}\text{Th}_x\text{Be}_{13}$  [38] as well as for layered dichalcogenides  $\text{CuS}_2$ ,  $\text{CuSe}_2$  and semimetallic superlattices  $\text{InAs–GaSb}$ ,  $\text{PbTe–SnTe}$  with geometrically separated bands belonging to different layers [37].

In the situation of a weak EPE for  $f_0^2 \ln m_h/m_L < 1$ ,  $Z_h \sim m_h/m_h^* \sim 1$  and  $\varepsilon_{Fh}^* \sim \varepsilon_{Fh}$ , and according to [15, 16], the maximal  $T_{C1}$  is given by

$$T_{C1} \sim \varepsilon_{Fh} \exp \left\{ -\frac{1}{2f_0^2 m_h/m_L} \right\}. \quad (87)$$

Therefore, the effective gas parameter that governs  $T_{C1}$  in case of a weak EPE is  $f_0(m_h/m_L)^{1/2}$ . At the same time, in the unitary limit for  $f_0 \rightarrow 1/2$  and  $m_h^*/m_L \sim (m_h/m_L)^2$ , the estimates show that

$$T_{C1} \sim \varepsilon_{Fh}^* \exp\{-1/2f_0^2\} \sim \varepsilon_{Fh}^* \exp\{-2\}. \quad (88)$$

It follows that for  $\varepsilon_{Fh}^* \sim 50$  K,  $T_{C1}$  can reach 5 K, which is quite nice.

When we increase the density of the heavy band and come closer to half-filling ( $n_h \rightarrow 1$ ), the  $d$ -wave SC pairing (as in  $\text{UPt}_3$ ) becomes more beneficial in the framework of the spin-fluctuation theory in the heavy band [40, 41]. The more exotic mechanisms of SC in heavy-fermion compounds including odd-frequency pairing [5, 42] are also possible.

We note that in the 2D case, where only the EPE effect is present for the mass enhancement of heavy electrons, the restrictions on the homogeneous case are milder than in 3D.

## 9. DISCUSSION AND CONCLUSIONS

We analyzed characteristic features of the two-band Hubbard model with one narrow band taking the electron–electron scattering into account in the clean case (no impurities) for low electron densities. We considered the electron polaron effect and other mechanisms of heavy mass enhancement related to the momentum dependence of self-energies.

In the 3D case, the dominant mechanism of heavy mass enhancement is related to the momentum dependence of the real part of a “heavy–light” self-energy and leads to a heavy mass renormalization that is linear in the mass ratio. In the 2D case, the dominant mechanism of heavy mass enhancement is the EPE, which leads to a logarithmic renormalization of the heavy particle  $Z$ -factor. In the unitary limit, if we start with  $m_h/m_L \sim 10$  for the bare-mass ratio in the LDA scheme, we can finish with  $m_h^*/m_L \sim 100$  due to many-body effects, which is quite natural for uranium-based HF systems.

The important role of the interband (“heavy–light”) Hubbard repulsion  $U_{hL}$  for the formation of a heavy mass  $m^* \sim 100m_e$  in a two-band Hubbard model was also emphasized in [34] for the  $\text{LiV}_2\text{O}_4$  HF compound.

For a large density mismatch  $n_h \gg n_L$ , we can see the tendency towards negative compressibility in the heavy band in the strong-coupling limit  $f_0^2 m_h p_{Fh} / m_L p_{FL} \gtrsim 1$  already at low densities, which can lead to a redistribution of charge between the bands and possibly to nanoscale phase separation in qualitative similarity with the results in [14]. The tendency towards phase separation at low electron fillings also manifests itself for the asymmetric Hubbard model (which involves Hubbard repulsion between heavy and light electrons) in the limit of strong asymmetry:  $t_h \ll t_L$  [35] between heavy and light bandwidths.

For equal densities of the heavy and light bands, the resistivity in a homogeneous state behaves in a Fermi-liquid fashion:  $R(T) \sim T^2$  at low temperatures  $T < W_h^*$  in both 3D and in 2D cases (where  $W_h^*$  is the effective bandwidth of heavy particles).

For higher temperatures  $T > W_h^*$ , when a coherent motion of particles in the heavy band is totally destroyed, the heavy particles move diffusively in the surrounding of light particles, while the light particles scatter on the heavy ones as if on immobile (static) impurities. The resistivity saturates in the 3D case, which is typical for some uranium-based HF-compounds including  $\text{UNi}_2\text{Al}_3$ .

In 2D, due to weak-localization corrections of the Altshuler–Aronov type, the resistivity at higher temperatures has a maximum and then a localization tail. Such behavior could also be relevant for some other mixed-valence systems possibly including layered manganites. A similar behavior with a metal-like low-temperature dependence of the resistivity for  $T < 130$  K and the insulator-like high-temperature dependence was also observed in layered intermetallic alloys  $\text{Gd}_5\text{Ge}_4$ , where the authors of [36] assume the existence of a strongly correlated narrow band at low temperatures.

We briefly discuss the SC instabilities that arise in this model at low electron densities. The leading instability of the enhanced Kohn–Luttinger type corresponds to  $p$ -wave pairing of heavy electrons via polarization of light electrons. In the quasi-2D case,  $T_C$  can reach experimentally realistic values already at low densities for layered dichalcogenides  $\text{CuS}_2$  and  $\text{CuSe}_2$  and semimetallic superlattices  $\text{InAs–GaSb}$  and  $\text{PbTe–SnTe}$  with geometrically separated bands belonging to neighboring layers [37]. We note that the  $p$ -wave SC is widely discussed in 3D heavy-fermion systems like  $\text{U}_{1-x}\text{Th}_x\text{Be}_{13}$  [38] and in layered ruthenates  $\text{Sr}_2\text{RuO}_4$  with several pockets (bands) for conducting electrons [39]. Also, when we increase the density of the

heavy band and come closer to half-filling ( $n_h \rightarrow 1$ ), the  $d$ -wave superconductive pairing (as in  $\text{UPt}_3$ ) becomes more beneficial in the framework of the spin-fluctuation theory in the heavy band [40, 41]. Different mechanisms of SC in HF-compounds including odd-frequency pairing are discussed in [42].

We also note that if we study the orbitally degenerate two-band Hubbard model, then the Hubbard parameters are  $U = U_{hh} = U_{LL} = U_{hL} + 2J_H$  (where  $J_H$  is Hund’s coupling) [43]. Close to half-filling, this model becomes equivalent to the  $t$ - $J$  orbital model [44] and for  $J < t$  and at optimal doping contains the SC  $d$ -wave pairing [45] governed by a superexchange interaction between different orbitals of the AFM type  $J > 0$ . For not very different values of  $t_h$  and  $t_L$ , the typical value of  $J$  is of the order of  $t^2/U \sim 300$  K. The orbital  $t$ - $J$  model also reveals a tendency towards nanoscale phase separation at low doping [46] with the creation of orbital ferrons inside the insulating AFM orbital matrix. An orbital type of phase separation was possibly observed in  $\text{URu}_2\text{Si}_2$  [47].

We are grateful to A. S. Alexandrov, A. F. Andreev, A. F. Barabanov, M. A. Baranov, Yu. Bychkov, A. V. Chubukov, D. V. Efremov, P. Fulde, A. S. Hewson, Yu. Kagan, K. A. Kikoin, K. I. Kugel, F. V. Kusmartsev, M. Mezard, Yu. E. Lozovik, P. Nozieres, N. V. Prokof’ev, A. L. Rakhmanov, T. M. Rice, A. O. Sboychakov, G. V. Shlyapnikov, P. Thalmeier, C. M. Varma, D. Vollhardt, P. Woelfle, and A. Yaresko for the numerous simulating discussions on this subject and acknowledge financial support of the RFBR grants №№ 08-02-00224, 08-02-00212. M. Yu. K. is also grateful to Loughborough University (UK) and LPTMS (Orsay, France) for the hospitality during the final stage of this work and acknowledges financial support from the Leverhulme trust and CNRS (contract № 236694).

## REFERENCES

1. C. M. Varma, P. B. Littlewood, S. Schmitt-Rink, E. Abrahams, and A. E. Ruchenstein, *Phys. Rev. Lett.* **63**, 1996 (1989).
2. Yu. Kagan and N. V. Prokof’ev, *Sov. Phys. ZhETP* **93**, 356 (1987); Yu. Kagan and N. V. Prokof’ev, *Sov. Phys. ZhETP* **90**, 2176 (1986).
3. B. L. Altshuler and A. G. Aronov, in: *Modern Problems in Condensed Matter Systems*, Vol. 10, p. 1, North Holland, Amsterdam (1985).
4. W. Kohn and J. M. Luttinger, *Phys. Rev. Lett.* **15**, 524 (1965).

5. J. Kondo, *Progr. Theor. Phys.* **32**, 37 (1964); C. M. Varma, and Y. Yafet, *Phys. Rev. B* **13**, 2959 (1976); A. C. Hewson, *The Kondo Problem in Heavy Fermions*, Cambridge University Press, Cambridge (1993); K. G. Wilson, *Rev. Mod. Phys.* **47**, 773 (1975); P. W. Anderson, G. Yuval, and D. R. Hamann, *Phys. Rev. B* **1**, 4464 (1970); P. Nozieres, *J. Low Temp. Phys.* **17**, 31 (1974).
6. A. M. Tsvelik and P. B. Wiegman, *Adv. in Phys.* **32**, 453 (1983); N. Andrei, F. Furuya, and J. H. Loerensstein, *Rev. Mod. Phys.* **55**, 331 (1983); P. Coleman, *Phys. Rev. B* **29**, 3035 (1984).
7. D. M. Newns and M. Read, *Adv. in Phys.* **56**, 799 (1987); P. Coleman, *Phys. Rev. B* **35**, 5072 (1987); H. Keiter and N. Grewe, in *Valence Fluctuations in Solids*, North Holland, New York (1981), p. 451; C. M. Varma, arXiv:cond-mat/0510019 (2005) and references therein.
8. J. S. Kim, B. Andraka, and G. R. Stewart, *Phys. Rev. B* **45**, 12081 (1992).
9. L. M. Falicov and J. C. Kimball, *Phys. Rev. Lett.* **22**, 997 (1969).
10. M. Yu. Kagan and A. G. Aronov, *Czechoslovac. J. Phys.* **46**, 2061 (1996), *Proc. of LT-21 Conference*, Prague (1996).
11. S. Watanabe, A. Tsumata, K. Miyake, and J. Flouquet, *J. Phys. Soc. Jpn.* **79**, 104706 (2009); K. Miyake, *J. Phys. Soc. Jpn.* **74**, 254 (2005).
12. F. C. T. O'Farrell, D. A. Tompsett, S. E. Sebastian et al., arXiv:cond-mat 08114417.
13. A. L. Rakhmanov, K. I. Kugel, Ya. M. Blanter, and M. Yu. Kagan, *Phys. Rev. B* **63**, 174424 (2001); M. Yu. Kagan and K. I. Kugel, *Usp. Phys. Sci.* **171**, 577 (2001); M. Yu. Kagan, D. I. Khomskii, and M. V. Mostovoy, *Eur. Phys. J. B* **12**, 217 (1999); K. L. Kugel, A. L. Rakhmanov, A. O. Sboychakov et al., *ZhETP* **98**, 572 (2004).
14. K. I. Kugel, A. L. Rakhmanov, and A. O. Sboychakov, *Phys. Rev. B* **76**, 195113 (2007).
15. M. Yu. Kagan and A. V. Chubukov, *JETP Lett.* **47**, 525 (1988); M. A. Baranov, A. V. Chubukov, and M. Yu. Kagan, *Int. J. Mod. Phys. B* **6**, 2471 (1992); M. A. Baranov, D. V. Efremov, M. S. Mar'enko, and M. Yu. Kagan, *ZhETP* **90**, 861 (2000); M. A. Baranov and M. Yu. Kagan, *Z. Phys. B* **86**, 237 (1992).
16. M. Yu. Kagan, *Phys. Lett. A* **152**, 303 (1991); M. A. Baranov and M. Yu. Kagan, *ZhETP* **102**, 313 (1991).
17. J. Kanamori, *Progr. Theor. Phys.* **30**, 275 (1963); J. Hubbard, *Proc. Roy. Soc. A* **276**, 235 (1963).
18. V. M. Galitskii, *ZhETP* **34**, 151 (1958).
19. E. M. Lifshitz and L. P. Pitaevskii, *Statistical Physics*, Part 2, Nauka, Moscow (1973).
20. P. Bloom, *Phys. Rev. B* **12**, 125 (1975).
21. A. A. Abrikosov, L. P. Gor'kov, and I. E. Dzyaloshinskii, *Methods of Quantum Field Theory in Statistical Physics*, Dover, New York (1975).
22. M. Yu. Kagan, *Superconductivity and Superfluidity in Fermi-Systems with Repulsive Interaction*, Habilitation Thesis, P. L. Kapitsa Institute for Physical Problems, Moscow (1994).
23. P. W. Anderson, *Phys. Rev. Lett.* **64**, 1839 (1990); **65**, 3306 (1990); **66**, 3226 (1991).
24. J. R. Engelbrecht and M. Randeria, *Phys. Rev. Lett.* **65**, 1032 (1990); **66**, 3225 (1990); J. R. Engelbrecht and M. Randeria, *Phys. Rev. B* **45**, 12419 (1992).
25. G. Iche and P. Nozieres, *Physica A* **91**, 485 (1978); P. Nozieres and L. T. de Dominicis, *Phys. Rev.* **178**, 1097 (1969).
26. P. W. Anderson, *Phys. Rev. Lett.* **18**, 1049 (1958); P. W. Anderson, *Phys. Rev. B* **164**, 352 (1967).
27. R. M. White and P. Fulde, *Phys. Rev. Lett.* **47**, 1540 (1981); G. Zwicknagl, A. Yaresko, and P. Fulde, *Phys. Rev. B* **68**, 052508 (2003); G. Zwicknagl, A. Yaresko, and P. Fulde, *Phys. Rev. B* **65**, 081103 (2002); M. Koga, W. Liu, M. Dolg, and P. Fulde, *Phys. Rev. B* **57**, 10648 (1998); P. Fulde, *Electron Correlations in Molecules and Solids*, Springer, Berlin (1995).
28. Yu. Kagan, K. A. Kikoin, and N. V. Prokof'ev, *JETP Lett.* **56**, 221 (1992).
29. I. M. Lifshitz and A. M. Kosevich, *Zh. Eksp. Theor. Phys.* **29**, 730 (1955); D. Schoenberg, *Magnetic Oscillations in Metals*, Mir, Moscow (1986); L. Taillefer and G. G. Lonzarich, *Phys. Rev. Lett.* **60**, 1570 (1988); A. Wasserman, M. Springford, and A. C. Hewson, *J. Phys. Cond. Matt.* **1**, 2669 (1989).
30. T. Ito, H. Kumigashira, H.-D. Kim et al., *Phys. Rev. B* **59**, 8923 (1999); A. J. Arko, J. J. Joyce, A. B. Andrews et al., *Physica B* **230-232**, 16 (1997).
31. A. Berton, J. Chaussy, B. Cornut et al., *Phys. Rev. B* **23**, 3504 (1981); G. R. Stewart, *Rev. Mod. Phys.* **56**, 755 (1984); H. R. Ott, *Progr. Low. Temp. Phys.* **11**, 215 (1987).
32. E. M. Lifshitz and L. P. Pitaevskii, *Physical Kinetics*, Nauka, Moscow (1979); L. D. Landau, *Phys. Zeitschr. Sow.* **10**, 154 (1936).

33. Y. Imry, *Introduction to Mesoscopic Physics*, Oxford University Press, Oxford (2002).
34. H. Kusunose, S. Yotsuhashi, and K. Miyake, *Phys. Rev. B* **62**, 4403 (2000).
35. P. Farkašovský, *Phys. Rev. B* **77**, 085110 (2008).
36. E. M. Levin, V. K. Pecharsky, K. A. Gschneidner, Jr., and G. J. Miller, *Phys. Rev. B* **64**, 235103 (2001).
37. K. Murase, S. Ishida, S. Takaoka et al., *Surf. Sci.* **170**, 486 (1986).
38. F. Kromer, R. Helfrich, M. Lang, and F. Steglich, *Phys. Rev. Lett.* **81**, 4476 (1998); M. Sigrist and K. Ueda, *Rev. Mod. Phys.* **63**, 239 (1991) and references therein.
39. Y. Maeno, T. M. Rice, and M. Sigrist, *Phys. Today* **54**, 42 (2001); T. M. Rice and M. Sigrist, *J. Phys.: Cond. Mat.* **7**, L643 (1995).
40. D. J. Scalapino, E. Loh, Jr., and J. E. Hirsch, *Phys. Rev. B* **34**, 8190 (1986).
41. K. Miyake, S. Schmitt-Rink, and C. M. Varma, *Phys. Rev. B* **34**, 6554 (1986).
42. P. Coleman, E. Miranda, and A. Tsvelik, *Phys. Rev. Lett.* **70**, 2960 (1993); R. Flint, M. Dzero, and P. Coleman, *Nat. Phys.* **4**, 643 (2008) and references therein; P. Coleman, in *Handbook of Magnetism and Advanced Magnetic Materials*, Vol. 1: *Fundamentals and Theory*, John Wiley and Sons, Hoboken (2007).
43. K. I. Kugel and D. I. Khomskii, *Usp. Phys. Sci.* **136**, 621 (1982).
44. S. Ishihara, J. Inoue, and S. Maekawa, *Phys. Rev. B* **55**, 8280 (1997).
45. M. Yu. Kagan and T. M. Rice, *J. Phys.: Cond. Mat.* **6**, 3771 (1994).
46. K. I. Kugel, A. L. Rakhmanov, A. O. Sboychakov, and D. I. Khomskii, *Phys. Rev. B* **78**, 115113 (2008).
47. P. Chandra, P. Coleman, J. A. Mydosh, and V. Tripathi, *Nature* **417**, 831 (2002); P. Chandra, P. Coleman, J. A. Mydosh, and V. Tripathi, *J. Phys.: Cond. Mat.* **15**, S1965 (2003).